Turbulent Coagulation Rate of Inclusion Particle and Morphology of Cluster in Molten Metal

	リ　タオ
氏　　名	李　涛
授　与　学　位	博士（環境科学）
学位記番号	環博第７７号
学位授与年月日	平成２５年３月２７日
学位授与の根拠法規	学位規則第４条第１項
研究科，専攻の名称	東北大学大学院環境科学研究科（博士課程）環境科学専攻
学位論文題目	Turbulent Coagulation Rate of Inclusion Particle and Morphology of Cluster in Molten Metal（溶融金属中介在物の乱流凝集速度とクラスターの形態に関する研究）
指導教員	東北大学教授　谷口　尚司
論文審査委員	主査　東北大学教授　谷口　尚司　　東北大学教授　葛西　栄輝 東北大学教授　北村　信也　　東北大学准教授　井上　亮 （多元物質科学研究所）　　（多元物質科学研究所）

論文内容要旨

Steel plays an important role in every aspect nowadays, such as buildings, railways, wire bridges, bearings, vehicles and so on. However, nonmetallic inclusions in steel have serious adverse effects on the steel products properties, such as strength, toughness, fatigue property, plasticity, surface smoothness and corrosion resistance. The requirements of the control and removal of inclusions in steel products become more and more serious with the increasing customer demands on the steel products performance.

The purpose of this study is to investigate particle coagulation mechanism in molten metal which plays a key role to remove inclusions in molten steel. However, it is rare to find experimental reports about the inclusion coagulation in molten metal since the lack of techniques to obtain the 3D information of the number, size, and structure of inclusion clusters in metal system which is indispensable to obtain the particle coagulation rate. Currently, the statistical analysis of inclusion and clusters in metal system is only based on the 2D cross sectional observation of as-polished samples. To obtain the quantitative statistics of clusters, it is required to distinguish clusters in 2D cross sectional images of as-polished samples, which is a tough but meaningful work. Furthermore, stereological analysis of particles and clusters included in a solid media serves as a bridge between the 2D and 3D statistics of the system. Therefore, it is necessary to obtain 3D information of particle and clusters in metal system to analyze the kinetics of particle coagulation in molten metal.

In this study, the theory of particle coagulation verified previously by water model experiments was investigated of its applicability to molten Al system. The experimental coagulation curve of SiC particles in molten Al stirred mechanically was found to shift to longer time compared with the calculated curve for various agitation speeds and particle concentrations. The reason of this discrepancy was attributed to the 2D measurement of particle and cluster size and number on the cross sections of solid metal, which was more uncertain than the electrical sensing zone method adopted in the water model study. Therefore, the 3D information of particle and cluster became crucial to obtain reliable data of coagulation curve. The main contents of this study are summarized as follows:

In Chapter 2, the theory of particle coagulation was investigated including previous study with water model experiments by Taniguchi et al. The PSG method recommended by Nakaoka greatly reduced the computation loads. The Hamaker constant of SiC particle in water was obtained by previous study which was used to estimate its value in liquid metal. It gives 0.61×10^{-20} J as the Hamaker constant of SiC in liquid Al, which is very important parameter for the calculation in Chapter 3. Particle coagulation experiments using TiB_2 particles were carried out to validate the particle coagulation theory. The experimental and calculated results of particle coagulation show a good agreement when Hamaker constant of TiB_2 particle in water is fitted as 0.88×10^{-20} J. The estimated Hamaker constant of TiB_2 particle in liquid Al is 4.62×10^{-20} J at 1073K.

In Chapter 3, particle coagulation experiments were carried out using SiC particles in molten Al. The average particle area fractions in the whole cross sectional microscopic images of all the samples taken from different positions in the crucible do not differ from the initial particle volume fraction in the system. The average particle area fractions in the whole cross section of microscopic images of samples taken from different time during agitation are almost kept as constant, which indicates the satisfactory balance in this analysis. A Java based program DC-2D was developed to distinguish clusters in the cross sectional images, which is corresponding to the human eyes' reliability in most cases. The relation between rotating impeller torque and energy dissipation rate in the bulk of fluid in agitated vessel was investigated through experiments and simulations and compared with the previous studies concerning the particle coagulation. The calculated results of SiC particle coagulation in molten Al shows a faster coagulation rate comparing with the experimental ones by using the Hamaker constant estimated in Chapter 2 and the turbulent dissipation rate investigated in this Chapter. **Figure 1** compares the experimental and calculated results of SiC particle coagulation in molten Al, where $n_k^* = n_{3D,k} / N_{0,3D}$ is dimensionless cluster number density; $t^* = 1.3\alpha a_1^3(\varepsilon/\nu)^{1/2} N_{0,3D} t$ is dimensionless time. The difference between the calculated and experimental results may be attributed to the lack of 3D information of particle and clusters in metal system. The overestimation of the 2D cluster sizes by the program of DC-2D and the assumed spherical shape of clusters with fractal dimension of 3.0 caused the calculated coagulation rate faster.

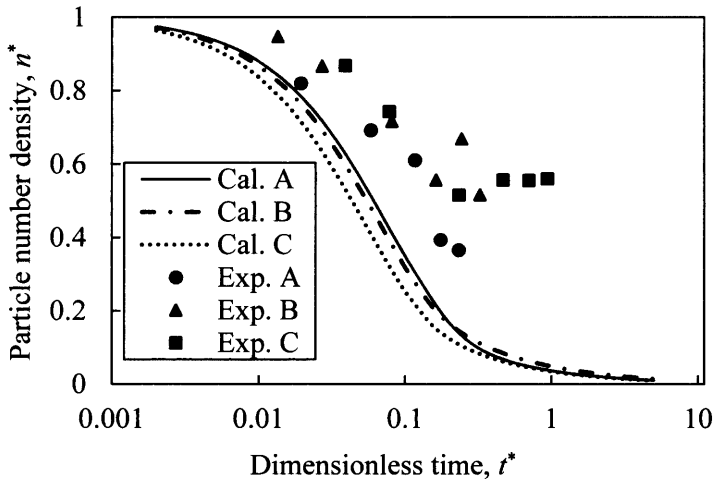

Figure 1. Change in cluster number with time (Dimensionless)

In Chapter 4, X-ray micro-CT was applied to obtaining the 3D information of clusters in metal. The principle of X-ray micro-CT was introduced. The X-ray mass attenuation coefficient decreases with the increasing energy of the photo beam. The difference of X-ray linear attenuation coefficients between Al matrix and SiC are very small. Therefore, it is very difficult to distinguish them by X-ray micro-CT. On the other hand, the

difference of the X-ray linear attenuation coefficients between Al matrix and TiB_2 is much larger than that of Al–SiC system. The detection of TiB_2 particles in Al matrix by X-ray micro-CT is not difficult. The size of Al–TiB_2 samples are determined as 0.8 mm in diameter exposed under the X-ray beam with energy of 19.99 keV; while the size of the samples of Al–SiC are 0.5 mm with 18ekV. A program was developed to pretreat the 8bit micro-CT images and reduce noises by considering the two slices before and after the present slice. The program of 3D Extractor was developed to extract particles and clusters from X-ray micro-CT image stacks; and parameters were defined to describe their size and structure in 3D and 2D. **Figure 2** shows an example of extracted 3D TiB_2 cluster and its 2D cross sectional slices.

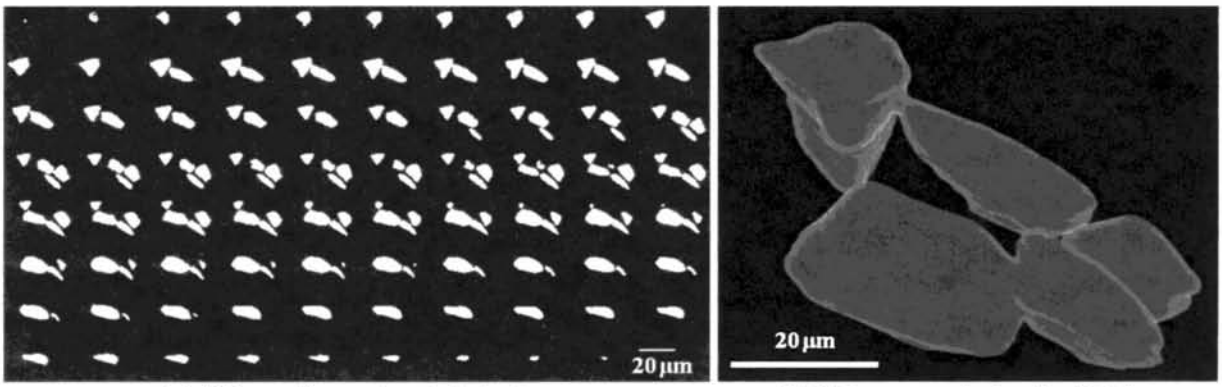

(a). Slices of an extracted cluster. (b). Volume rendering by Osirix.

Figure 2. Slices of an extracted cluster and 3D reconstruction.

In Chapter 5, a stereological model was introduced to investigate the relation of 2D cross sectional and 3D information of particles dispersed in solid metal. The particle size distribution (PSD) of nonspherical TiB_2 powder was analyzed by optical microscopy and Coulter Counter-3. The PSD-P and the 3D PSD were compared. They showed good agreement when the fractal dimension of a single particle was taken to be 2.7. 3D images of single particles were reconstructed from a series of micro-CT images obtained by X-ray micro-CT at SPring-8. This enabled to determine the complete shapes of nonspherical particles. The fractal dimension D_f^* of a particle was calculated from its volume and the maximum diameter of the X, Y, and Z coordinates. Particles were divided into three groups and dominant particles were found to have a D_f^* in the range 2.6–2.8. The probability mass functions (PMFs) of the dominant particles showed the same tendency and differed greatly from that of a spherical particle. The PMFs of randomly selected dominant particles and their average PMF were used in the stereological calculation model. The transformation from 3D PSD to 2D PSD-C (cross section) was established based on the stereological model by assuming that all the particles in a nonspherical particle system have the same shape and PMF. Good agreement was obtained within a tolerance of statistical and systematic errors. The inverse problem occurred in the transformation of PSD from 2D PSD-C to 3D PSD. It could be overcome by introducing a system error analysis, increasing the number of classes, and adjusting the range of classes to obtain a compatible PMF matrix. The Santalo equation employing 2D average cluster diameter is the only way to estimate the cluster number density per unit volume unless solving inverse problem occurred in the transformation from 2D to 3D information.

In Chapter 6, TiB_2 particles were used to obtain clusters in an agitated crucible. The 3D parameters of TiB_2 clusters were analyzed to describe the 3D characteristics of the clusters. It was difficult to observe the coagulation kinetics of TiB_2 particle in molten Al because the coagulation tendency was very weak. This

might because the contact angle of TiB_2 particle in molten Al is small comparing with SiC. A number of TiB_2 clusters were extracted by the program of 3D Extractor. The 3D cluster structure was not affected by the agitation time and speed. Whereas the particle number included in the clusters affects more on their structure. The specific surface and solidity decrease greatly with particle number in the clusters, which indicates the clusters become looser with the increase of particle number. There is not apparent change for 3D parameters of cluster structure with the increasing of particle number in the clusters. It can be roughly concluded that the fractal dimension of TiB_2 clusters formed in molten Al is around 2.7. The 2D fractal dimension of TiB_2 clusters is around 1.8. The relation between the 3D and 2D fractal dimensions is corresponding to that between 3D and 2D for spheres (3.0 and 2.0). The 2D clusters were successfully distinguished by the program of DC-2D-3D according to the 2D parameters of cluster slices obtained from the actual 3D clusters.

In Chapter 7, the X-ray micro-CT images of Al–SiC system were treated by phase retrieval based on FFT, which largely removed noise in the X-ray micro-CT images of Al–SiC system. ImageJ was applied to enhance the contrast of 8-bit images. 3D SiC particles and clusters were extracted from a series of X-ray micro-CT image stacks by the program of 3D Extractor. The 3D parameters describing the structures of SiC clusters are similar to that of TiB_2 clusters. It can be concluded that the fractal dimension of both SiC and TiB_2 clusters are around 2.7, which can be applied to improve the coagulation theory. The program of DC-2D-3D including criterions obtained from actual clusters was applied to Al–SiC system on microscopy images. **Figure 3** compares the cluster distinguished by program of DC-2D and DC-2D-3D. It seems that the cluster distinguished by program of DC-2D-3D is much more reasonable than that by DC-2D. The kinetics of SiC particle coagulation in molten Al was recalculated according to the results by DC-2D-3D programs. The fractal dimension of clusters is also considered. The agreements between experimental results and theory were greatly improved shown in **Figure 4**.

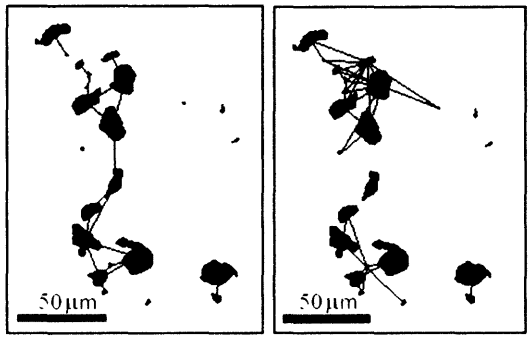

Figure 3. Comparison of clusters distinguished by program of DC-2D and DC-2D-3D.

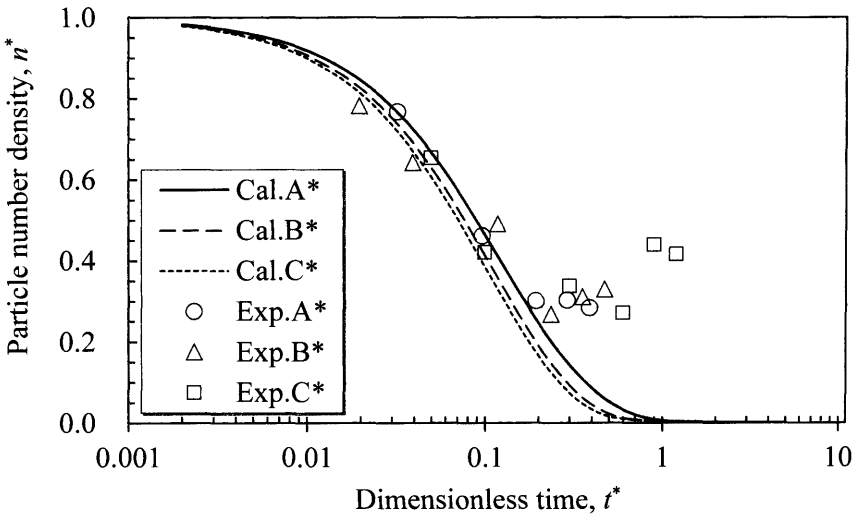

Figure 4. Improved SiC particle coagulation results by program of DC-2D-3D.

論文審査結果の要旨

溶融金属中には多数の非金属介在物粒子が存在するが、大型の介在物が凝固時に残留すると製品の性能や品質を大きく害する。一方、溶融金属を攪拌して介在物を積極的に凝集・肥大化させることにより、介在物の分離・除去が容易になる。このように、溶融金属中介在物の凝集現象は、金属製品の清浄化に関係する極めて重要な現象である。これまで水中の粒子の凝集については、攪拌槽を用いた乱流凝集実験によりその機構が解明されている。しかし溶融金属中の介在物凝集については、介在物の大きさと個数の正確な評価が困難で、測定上の問題すら解決されていない状況にある。本論文は、溶融アルミニウム中で乱流凝集したSiC粒子に対して、X線マイクロCT法による3次元粒子構造解析を行い、これにより介在物凝集の定量的な測定と解析を可能にしたもので、全編8章よりなる。

第1章は緒論であり、本研究の背景と目的について述べている。

第2章では、水中粒子の乱流凝集に関する既往の研究について概説し、一例としてAl合金製造において重要なTiB_2粒子に着目し、その水中での凝集に既往の乱流凝集モデルが適用できることを明らかにしている。

第3章では、すでに得られているSiC粒子の溶融Al中における粒子間Hamaker定数（van der Waals力の定数）の推算値を用いて、攪拌下のSiC粒子の凝集曲線（粒子全濃度と時間との関係）の理論値を求め、実験結果と比較している。凝集曲線の実験値は計算値より長時間側に位置しており、両者の間に明らかな差異が認められた。この差異が、粒子径および粒子濃度を2次元断面観察で求める方法の問題に起因することを明らかにしている。

第4章では、SPring-8の高輝度放射光を利用したX線マイクロCT法を、Al中のSiC粒子およびTiB_2粒子の3次元形態解析に利用するための測定条件を検討し、TiB_2粒子がSiC粒子に比して測定に適することを示している。

第5章では、Al中に分散したTiB_2の単独粒子のCT画像から、粒子の2次元断面像と3次元像とを理論的に関係づけ、$V=\pi d^{D_f}/6$（Vは粒子体積、dは粒子の平均径）で与えられるフラクタル次元D_fが約2.7であることを示した。この結果から2次元断面の面積相当径と、コールター原理による体積相当径との関係を明らかにしている。

第6章では、Al中のTiB_2クラスターのCT画像から、クラスター粒子の構造に関係するフラクタル次元、比表面積、空間充填率などを求め、それらの諸量とクラスターの構成粒子数との関係を解析した。その統計情報を判定基準として、試料断面の顕微鏡写真よりクラスターを識別する手法を提案している。

第7章では、Al中のSiCクラスターの不鮮明なCT画像に、最新の画像処理技術を適用して鮮明化した画像を用いて、前章のTiB_2クラスターの解析と同様の解析を行うことにより、第2章のSiC粒子の乱流凝集実験結果を改めて解析し直した。その結果、凝集曲線の理論値と実験値との差異は解消し、水モデル実験を対象に展開された凝集理論が溶融金属系に対しても適用できることを明らかにしている。

第8章は総括である。

以上要するに、本論文は金属中介在物粒子の3次元のクラスター構造と2次元のそれとの関係を明らかにし、これによって既往の乱流凝集理論が溶融Al中のSiC粒子凝集に適用できることを示したもので、金属材料の清浄化技術の進展に寄与するところが少なくない。

よって，本論文は博士(環境科学)の学位論文として合格と認める。